SUPERSEDING MODEL SCALING BY PENALIZING DEAD UNITS AND POINTS WITH SEPARATION CONSTRAINTS

Anonymous authors
Paper under double-blind review

ABSTRACT

In this article, we study a proposal that enables to train extremely thin (4 or 8 neurons per layer) and relatively deep (more than 100 layers) feedforward networks without resorting to any architectural modification such as Residual or Dense connections, data normalization or model scaling. We accomplish that by alleviating two problems. One of them are neurons whose output is zero for all the dataset, which renders them useless. This problem is also known as *dead neurons*. The other is a less studied problem, *dead points*. Dead points refers to data points that are mapped to zero during the forward pass of the network. As such, the gradient generated by those points is not propagated back past the layer where they die, thus having no effect in the training process. In this work, we characterize both problems and propose a constraint formulation that added to the standard loss function solves them both. As an additional benefit, the proposed method allows to initialize the network weights with constant values or even zero and still allowing the network to converge to reasonable results. We show very promising results on a toy, MNIST, and CIFAR-10 datasets.

1 INTRODUCTION

The success of Deep Neural Networks (DNN for short) is linked to its ability to learn *abstract representations* from input data in a hierarchical fashion (LeCun et al. (2006); Ramachandran et al. (2017)). However, the concepts of depth and width in networks are often used as instrumental elements to address different DNN pathologies during the learning process. Examples of these are: *vanishing gradient* (Hochreiter (1991; 2001)), *exploding gradient* (Pascanu et al. (2013)), *dead units* (Maas (2013); Douglas & Yu (2018); Guerraoui et al. (2017)), or the *degradation problem* (He et al. (2015b)).

In order to address the former issues, we find many methods and techniques that we can roughly classify in two families: *data manipulation* and *architectural modifications*. The most commonly used data manipulation technique is data normalization on the output of the layers, for example using batch normalization (Ioffe & Szegedy (2015)). Examples of architectural modifications include the use of additional connections, as done in ResNets (He et al. (2015b)) or DenseNets (Huang et al. (2016)); unit augmentation, as in *leaky*-`ReLU` (Maas (2013)), `PReLU` (He et al. (2015a)), `C-ReLU` (Shang et al. (2016)), or linked neurons (Riera & Pujol (2017)); or the increment of layer's width with depth (Zagoruyko & Komodakis (2016); Szegedy et al. (2014)). This last widely used approach effectively increases the the size of the network requiring larger computational power. This has led to several works (Hasanpour et al. (2018); Tan & Le (2019)) that address it by offering heuristics on how to scale the network. Recent research (Liu et al. (2018)) suggests that this inverted pyramidal architecture is not optimal.

Besides of the width scaling strategy, the concept of dead units[1] is of particular interest to this work. A dead neuron is defined as the neuron with a constant or zero output for all training data points. This effectively renders this unit ineffective during the learning process. In (Lu et al., 2019) it is shown that as the depth increases the probability of finding dead neurons also increases, to the point

[1] In this work we use *unit* and *neuron* indistinctly.

that the entire network can be dead even at initialization. Additionally, as expected, as the width of a layer increases, the probability of having dead neurons decreases.

In this article we characterize another pathology, the dead point. The dead point is a dual concept to the dead neuron. A dead point corresponds to a data point that does not reach the output of the network. This is, the activation is zero for all the units in a given layer. As a result, this data point will have no influence in the training process. As in the case of dead units, both condition are not recoverable by back-propagation. This virtually reduces the size of the training set.

In order to solve the former issues, we propose and present a geometrical optimization constraint that is added to the loss function. As a result of adding this constraint we ensure that all neurons are active and no points are dead. The rationale behind the geometrical constraint is to control that all units/neurons and data points are alive by constraining pre-activation values in such a way that the hyperplanes associated to the non-linearity of each RELU neuron separates, at least, one data point from the rest of the dataset. This has the additional effect of enabling the learning process to propagate all information through all the network avoiding the instrumental need of using additional connections or inverted pyramidal architectures.

We test our proposal in a series of controlled experiments to showcase the effect of applying the proposed *Separation Constraints*. We find that we can arbitrarily increase the network depth using the same constant width when compared to standard feedforward network and Batch Normalization Ioffe & Szegedy (2015) networks even when the width of the layer is extremely small (4 or 8 neurons). We additionally provide evidences that using this same approach we can initialize network parameters to zero and still achieve reasonable performance. These promising results gives insight on learning dynamics and suggest potential lines for future checks and research.

The article is organized as follows: Section 2 introduce the characterization of dead neurons and dead points, Section 3 introduces the two geometrical constraints that ensure that neurons and data points are alive, Section 4 describes the experiments and result, and, finally, Section 5 concludes the paper and suggests future lines of research.

2 CHARACTERIZING DEAD NEURONS AND DEAD POINTS

A standard feed-forward `ReLU` DNN (LeCun et al., 2015) F can be formally written as a multi-valued real function, $F(\mathbf{x})$, that is created by composing a collection of D vector *layer* functions $\ell : \mathbb{R}^{n_{k-1}} \to \mathbb{R}^{n_k}$. Layer k is defined as the sum of a collection of scalar functions (*units*):

$$\ell_k(\mathbf{x}) = \sum_{j=1}^{n_k} u_j^k(\mathbf{x})\hat{\mathbf{e}}_j \tag{1}$$

that affinely depend on a weight vector $\mathbf{w}_j^k \in \mathbb{R}^{n_k}$ and a bias parameter $b_j^k \in \mathbb{R}$. When using rectified linear units this value is truncated on negative values:

$$u_j^k(\mathbf{x}) = \max(0, \mathbf{w}_j^k \cdot \mathbf{x} + b_j^k). \tag{2}$$

Considering the hyperplane defined by $\mathbf{w}_j^k \cdot \mathbf{x} + b_j^k = 0$, each unit defines a partition of the space $\mathbb{R}^{n_k}$ in two sets: the *upper* part of unit u_j^k and the *lower* part of u_j^k:

$$\begin{aligned} upper(u_j^k) &= \{\mathbf{x} : \mathbf{w}_j^k \cdot \mathbf{x} + b_j^k > 0\} \\ lower(u_j^k) &= \{\mathbf{x} : \mathbf{w}_j^k \cdot \mathbf{x} + b_j^k \leq 0\} \end{aligned} \tag{3}$$

We define the *affine* component of a layer function ℓ_k as the intersection of the upper parts of its units, and its zero set as the intersection of the lower parts, as follows:

$$A(\ell_k) = \bigcap_{j=1}^{n_k} upper(u_j^k), \quad Z(\ell_k) = \bigcap_{j=1}^{n_k} lower(u_j^k) \tag{4}$$

Remark 2.1 (Dead unit)**.** *In a given `ReLU`-DNN $F : \mathbb{R}^n \to \mathbb{R}^k$, we say that the j-th unit of layer ℓ_k, u_j^k is* dead *with respect to a data set $\mathbb{X} \subset \mathbb{R}^{n_k}$ if and only if*

$$\mathbb{X} \subset lower(u_j^k). \tag{5}$$

Observe that if a unit is dead, the output of the unit will be zero for the entire dataset, rendering the unit useless. Moreover, since the gradient is zero as well, it remains in this state for the rest of the training (See Lu et al. (2019); Shin & Karniadakis (2019)). This effectively reduce the network learning capacity.

Remark 2.2 (Dead point with respect to a layer)**.** *Given* `ReLU`*-DNN* $F : \mathbb{R}^n \to \mathbb{R}^k$*, we say that a point* $\mathbf{x} \in \mathbb{X}$ *is* dead *with regards to layer* ℓ_k *if*

$$\mathbf{x} \in Z(\ell_k). \tag{6}$$

Remark 2.3 (Dead point)**.** *In particular, if* $\mathbb{X} \subset \mathbb{R}^n$*, we say that point* $\mathbf{x} \in \mathbb{X}$ *is* dead *with respect to a network* F *with depth* D *if it gets mapped to the zero set of a layer in its transit through the network. This is*

$$(\exists k, 1 < k \leq D | \ell_{k-1} \circ \dots \ell_1(\mathbf{x}) \in Z(\ell_k)). \tag{7}$$

Any dead point fulfilling Equation 7 will show zero gradient in the layers previous to ℓ_k. This hinders the learning process by effectively reducing the data set size. Again, this condition is not reversible using standard back-propagation. In a similar fashion to the case with dead units, the probability of finding a dead point increases with network's depth and decreases with layer's width.

3 Introducing separability constraints

In this section we introduce the desiderata for units and points to remain alive. Then, we proceed to formulate the separability contraints that fulfill the desired conditions.

Let us introduce the concept of a *separating* unit with respect to an arbitrary set $\mathbb{X}$.

Definition 3.1 (Separating Unit)**.** *Given an arbitrary set* $\mathbb{X} \subset \mathbb{R}^{n_k}$*, we say that the* j*-th unit on layer* k*,* u_j^k*, is able to* separate *through* $\mathbb{X}$ *if the following predicate is satisfied:*

$$R_{\mathbb{X}}(u_j^k) \equiv \emptyset \neq \{lower(u_j^k) \cap \mathbb{X}\} \subset \mathbb{X} \tag{8}$$

Thus, by construction, a separating unit can not be dead, and if $R_{\mathbb{X}}(u_j^k)$ is valid, u_j^k can not degrade set $\mathbb{X}$ to zero. In other words, this condition ensures that each unit always separates at least one data point.

In terms of points, we can define a *separating point* as follows:

Definition 3.2 (Separating point)**.** *Given an arbitrary set* $\mathbb{X} \subset \mathbb{R}^{n_k}$*, we say that point* $\mathbf{x} \in \mathbb{X}$ *is* separating *a layer function* ℓ_k *if there exist indices* $j, l \in \{1, \dots, m_k\}$ *for which the following predicate is satisfied.*

$$R_k^x(j, l) \equiv x \in \{upper(u_j^k) \cap lower(u_l^k)\} \tag{9}$$

Again, by construction, a separating point ensures that each point in the data set has at least one unit in each layer with an activation different to zero and another with an activation equal to zero.

3.1 Modelling Unit-based Separation Constraint (`Sep-U`)

Unit based separation contraint (`Sep-U`) is designed to model predicate 8 with the goal of avoiding the presence of dead units.

Given a unit u_j^k in layer $\ell_k : \mathbb{R}^{n_k} \to \mathbb{R}^{n_{k+1}}$ from a `ReLU` DNN F of depth D, predicate 8 can be simply modelled imposing the following constraints,

$$\begin{aligned} \max_{i=1,\dots,|\mathbb{X}|} \{\mathbf{w}_j^k \cdot \mathbf{x}_i + b_j^k\} > 0 \\ \min_{i=1,\dots,|\mathbb{X}|} \{\mathbf{w}_j^k \cdot \mathbf{x}_i + b_j^k\} < 0 \end{aligned} \tag{10}$$

These strict inequalities can not be directly optimized. It is easily to see that these can be rewritten as

$$\begin{aligned} &\max_{i=1,\ldots,|\mathbb{X}|} \{\mathbf{w}_j^k \cdot \mathbf{x}_i + b_j^k\} \geq 1 \\ &\min_{i=1,\ldots,|\mathbb{X}|} \{\mathbf{w}_j^k \cdot \mathbf{x}_i + b_j^k\} \leq -1 \end{aligned} \tag{11}$$

The use of the former constraints makes most problems unfeasible. Thus, in a similar fashion to soft-margin SVM (Cortes & Vapnik, 1995), we introduce a set of positive slack variables $\{\xi_{jk}^+, \xi_{jk}^-\}$ that account for constraint violations as follows,

$$\begin{aligned} &\max_{i=1,\ldots,|\mathbb{X}|} \{\mathbf{w}_j^k \cdot \mathbf{x}_i + b_j^k\} \geq 1 - \xi_{jk}^+, \\ &\min_{i=1,\ldots,|\mathbb{X}|} \{\mathbf{w}_j^k \cdot \mathbf{x}_i + b_j^k\} \leq -1 + \xi_{jk}^-, \\ &\xi_{jk}^+, \xi_{jk}^- \geq 0, \end{aligned} \tag{12}$$

for $k = 1, \ldots, D$ and n_k the number of units of layer k. The intuition behind the introduction of these constraints is as follows: by minimizing ξ^+ at least one pre-activation value is forced to be greater (or equal) than 1. Simmetrically, minimizing ξ^- promotes at least one pre-activation to be below -1. This effectively fulfills Predicate 8 and penalize the apparition of dead units.

At a global network scale, we can aggregate all the slack variable in a single optimization objective as follows,

$$g_U(\boldsymbol{\xi}^+, \boldsymbol{\xi}^-) = \frac{1}{2} \sum_{k=1}^{D} \sum_{j=1}^{n_k} (\xi_{jk}^+ + \xi_{jk}^-). \tag{13}$$

3.2 Modelling Point Based Separation Constraint (Sep-P)

The derivation of the Point Based Separation Constraints (Sep-P) follows a parallel process to Sep-U. In order to avoid the presence of dead points it suffices to fulfill Predicate 9. Similarly to the former derivation, we introduce a set of slack variables for each each point on the batch. That is, given $\mathbf{x}_i \in \mathbb{X}$, and $u_1^k, \ldots, u_n^k$ unit functions in a layer ℓ_k, we define slack variables ξ_{ik}^-, ξ_{ik}^+ in the context of the following constraints,

$$\begin{aligned} &\max_{j=1,\ldots,n_k} \{\mathbf{w}_j^k \cdot \mathbf{x}_i + b_j^k\} \geq 1 - \xi_{ik}^+, \\ &\min_{j=1,\ldots,n_k} \{\mathbf{w}_j^k \cdot \mathbf{x}_i + b_j^k\} \leq -1 + \xi_{ik,}^- \\ &\xi_{jk}^+, \xi_{jk}^- \geq 0. \end{aligned} \tag{14}$$

Observe that the minimization of the slacks makes that for any data point at least one activation is above 1 and another is below -1.

We can summarize all the point-based slack variables in a single optimization objective as follows,

$$g_P(\boldsymbol{\xi}^+, \boldsymbol{\xi}^-) = \frac{1}{2} \sum_{k=1}^{D} \sum_{i=1}^{|\mathbb{X}|} (\xi_{ik}^+ + \xi_{ik}^-). \tag{15}$$

3.3 Training with Separating Constraints

The new optimization objectives can now be added to the original loss objective using a simple scalarization (Boyd & Vandenberghe (2004)) as follows,

$$\arg\min_{\theta, \xi^+, \xi^-} \mathcal{L}(\mathcal{T}, \theta) + \lambda \big(g_U(\boldsymbol{\xi}^+, \boldsymbol{\xi}^-) + g_P(\boldsymbol{\xi}^+, \boldsymbol{\xi}^-) \big), \tag{16}$$

where λ is a hyper-parameter that introduces a trade-off between the constraint fulfillment and the main loss function.

In terms of memory *complexity*, the former constraints introduce a very small memory overhead. In particular, Sep-U places a pair of constraints on each of the units of the network, so the complexity with respect to Sep-U scales with the size of the network as $2 \sum_{k=1}^{D} n_k$. Alternatively,

Sep-P places a pair of constraints in each of the points of the data set or selected subset $\mathbb{X}$. In practice, one can use $\mathbb{X}$ as the training batch. Thus, the memory complexity scales with the size of the batch and the number of layers, i.e. $2D|\mathbb{X}|$. Furthermore, since the resulting gradient of both types of constraints depends only on the input of the layer that is already computed in the forward pass, we only add the cost of storing the slacks. Therefore, the total cost in terms of number of constraint is the addition of the former terms, i.e. $2\sum_{k=1}^{D} n_k + 2D|\mathbb{X}|$.

4 Experiments and Results

In this section we explore the application of the proposed constraints in different datasets. For that task we train all methods with different choices of depth and width parameters. The network architecture used is *rectangular*, i.e. networks with a fixed layer width for all the layers.

Datasets: Due to the large amount of computational resources required for the depth and width grid training, we are forced to chose three controlled datasets in our experimentation: the MOONS dataset (sampling 100 points, 85 for training and 15 for validation), the MNIST dataset as described in LeCun and Cortes. LeCun & Cortes (2010) and the CIFAR-10 dataset described in Krizhevsky (2009).

Experimental setting: We compare the combination of Sep-U and Sep-P (Sep-UP from now on) to feed-fordward ReLU networks (Glorot et al., 2011) and Batch Normalization as described in Ioffe & Szegedy (2015) using the same architecture.

For the MOONS dataset, we use depths from 1 to 120 in steps of 10, and width from 1 to 25 in steps of 1 between 1 and 5, and steps of 5 afterwards. In the case of the MNIST dataset, we use depth from 2 to 64 and width from 2 to 8 in steps of 4. Finally, for CIFAR-10 we use depths in $\{2, 10, 25, 30, 40\}$ with a fixed width of 10 due memory constraints.

Training Parameters: All the networks used were optimized using Adam (Kingma & Ba, 2014). More specifically, for the MOONS dataset we used a learning rate of 0.01 for 5000 epochs and a batch size of 85. Meanwhile, for both MNIST and CIFAR-10 we used a learning rate of 0.0001 for 50 epochs and a batch size of 1024. We used $\lambda_{MOONS} = 10^{-4}$ $\lambda_{MNIST} = \lambda_{CIFAR} = 10^{-8}$ for Sep-UP . Our experiments were conducted using Keras (Chollet et al., 2015) and TensorFlow (Abadi et al., 2015), fixing the random seed to an arbitrary value of 10.

As initialization scheme, we used Glorot uniform from Glorot & Bengio (2010) for all the methods and datasets.

4.1 Results

Figure 1 shows the results obtained in the MOONS dataset. Our proposal Sep-UP is able to train networks successfully without increasing the width up to 60 layers deep (see Figures 1c and 1f), while ReLU breaks down at only 30 layers (see Figures 1a and 1d) and ReLU + BN suffers from severe accuracy degradation (see Figures 1b and 1b).

Observe that no configuration with lower width than 2-3 is successful in achieving maximum accuracy. We understand that there exists a minimum width required and this is related to the complexity of the problem. When using wider layers, the rest of the width is instrumentally used to enable the training of deeper networks. As previously commented, the larger the layer's width, the higher the chances of finding active units that do not cause dead points and dead units during initialization. In opposition, Sep-UP succesfully overcomes that constraint.

Notice that though Sep-UP is superior to all its competitors, it starts showing performance degradation after reaching depth 60 with the minimum width of 3. Considering that the number of parameters increases with the depth and width of the network and that we have a finite number of trained epochs, we conjecture that the displayed degradation is strictly due to the lack of convergence of the constrained network.

The separation constraint also proves successful on convolutional networks, as tested in MNIST and CIFAR-10 datasets. Figure 2 shows a similar behaviour to the MOONS dataset (Figure1). ReLU breaks down after a few layers, ReLU + BN delays the degradation of accuracy, while

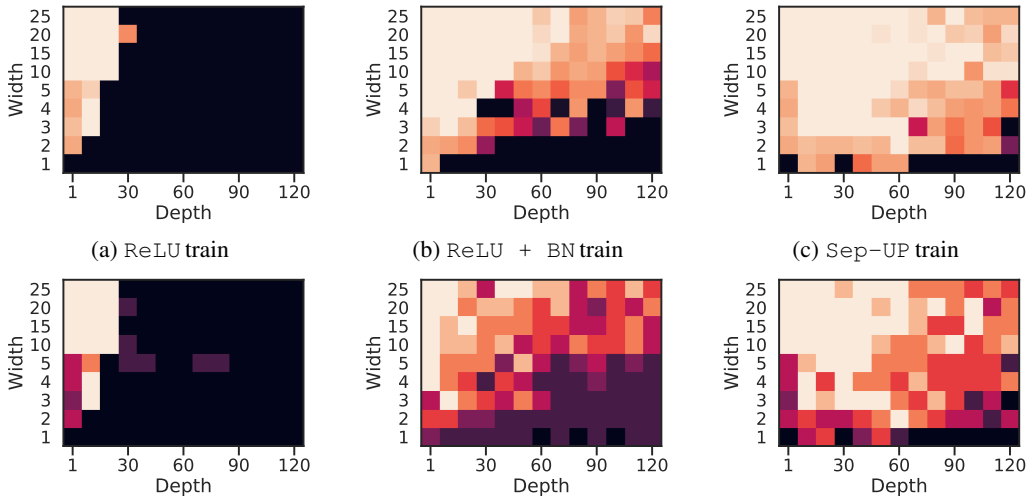

(a) ReLU train (b) ReLU + BN train (c) Sep-UP train

(d) ReLU validation (e) ReLU + BN validation (f) Sep-UP validation

Figure 1: Depth vs width accuracy heatmap a for a grid of rectangular networks with width from 1 to 25 and depth from 1 to 120, trained using Adam with a learning rate of 0.01 in the MOONS dataset for 5000 epochs. The color shows the accuracy attained of each of the combinations of width and depth, with clear beige at 1 and black at 0.5. Notice how ReLU breaks down at 20 layers and ReLU + BN requires more units per layer as increasing depth, while Sep-UP works with the minimum width (3) up to 60 layers deep.

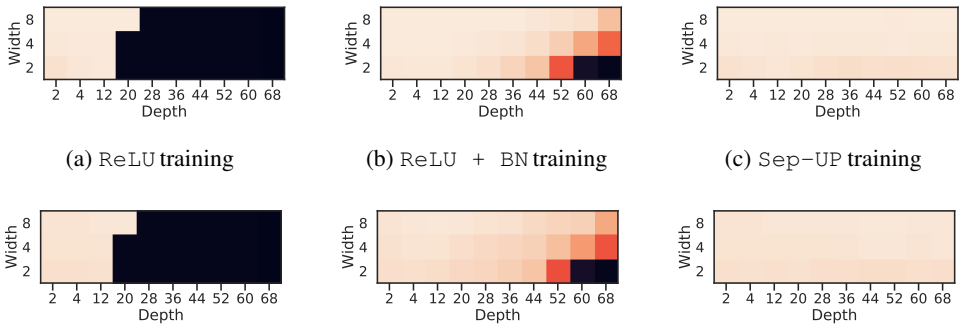

(a) ReLU training (b) ReLU + BN training (c) Sep-UP training

(d) ReLU validation (e) ReLU + BN validation (f) Sep-UP validation

Figure 2: Depth vs width accuracy heatmap a for a grid of rectangular networks with width from 2 to 8 and depth from 2 to 68, trained using Adam with a learning rate of 0.0001 in the MNIST dataset for 50 epochs. The color shows the accuracy attained of each of the combinations of width and depth, with clear beige at 1 and black at 0.1. Notice how ReLU breaks down at 20 layers and ReLU + BN accuracy degrades with depth, while Sep-UP shows constant accuracy disregarding the number of layers.

Sep-UP remains functional regardless of the depth. In the case of our experiments with the CIFAR-10 dataset (as presented on Figure 3) all the methods degrade with depth, but Sep-UP is the most robust. In regards to accuracy ReLU performs best closely followed by Sep-UP , while ReLU + BN clearly overfits. The poorer accuracy values shown are due to a limited choice of width, clearly inferior to the minimum required by the dataset, and a potential lack of convergence of the separating constraints.

Additional results in the Appendix further elaborate the contributions of each term Sep-U and Sep-P , independently.

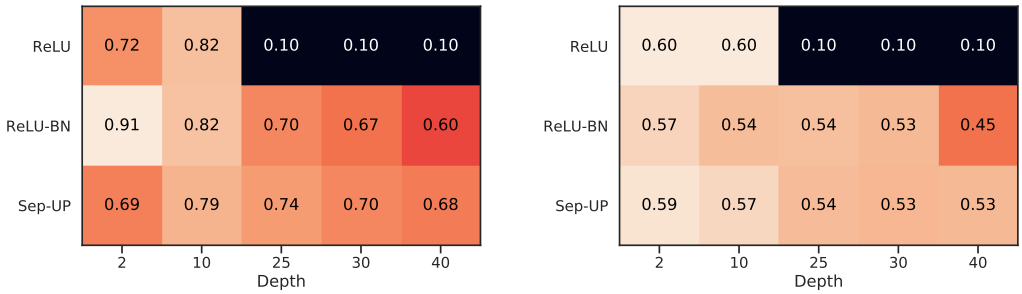

(a) Training accuracy

(b) Validation accuracy

Figure 3: Depth vs Width accuracy heatmap a for a grid of rectangular networks with width 10 and depth from 2 to 40, trained using `Adam` with a learning rate of 0.0001 in the `CIFAR-10` dataset for 50 epochs. The color shows the accuracy attained of each of the combinations of width and depth, with clear beige at 1 and black at 0.1. Observe how `Sep-UP` shows inferior degradation in accuracy as depth increases compared to `ReLU + BN`.

4.2 Results using Zero Initialization

In order to test the invariace to initialization scheme of `Sep-UP` , we use Zero Initialization. As its name states, in this initialization scheme all weights and biases are set to zero. However, a small variation of the scheme must be introduced in order to break symmetry for the constraints to apply. Since all the units are initialized to the same value (zero), we use Annealed Dropout (Rennie et al., 2014). Additionally, instead of adding ξ^+ and ξ^- pairs as in Equations 13 and 15, we use a convex combination with a small perturbation ρ. In our experiments, we use a value of $\rho = 0.01$.

$$(\frac{1}{2} + \rho)\xi^+ + (\frac{1}{2} - \rho)\xi^- \tag{17}$$

Figure 4 shows the results using this scheme. Although the reported values and behavior are slightly worse than using Glorot initialization, the results are promising. Notice how it requires a width of 25 units for a depth of 60 versus only 2 for Glorot to achieve maximum performance, see Figures 1c and 1f). However, compared to `ReLU + BN` , zero initialized network show a superior performance and behavior (check Figures 1b and 1e).

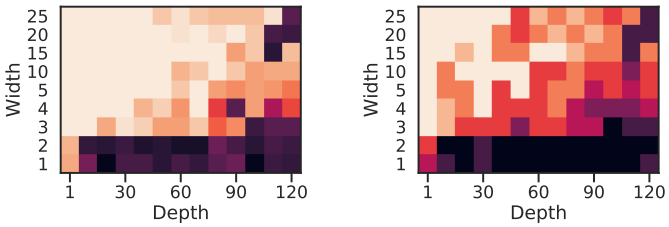

(a) `Sep-UP Zero-init` train

(b) `Sep-UP Zero-init` val.

Figure 4: Depth vs width accuracy heatmap a for a grid of rectangular networks with width from 1 to 25 and depth from 1 to 120, trained using `Adam` with a learning rate of 0.01 in the `MOONS` dataset for 5000 epochs and Zero Initialization. The color shows the accuracy attained of each of the combinations of width and depth, with clear beige at 1 and black at 0.5. Notice how although being inferior to Glorot (Figures 1c and 1f) is superior to `ReLU + BN` (Figures 1b and 1e).

5 CONCLUSIONS

Through the Separation Constraints, we have shown that deeper networks can be trained without increasing the width of the layers. Moreover, this increment can be done using very small width values. In this sense we consider that effective training of deeper networks can be achieved by better accommodating the network to the input data. This departs from many proposal that achieve similar effects by modifying the architecture of the network or manipulating the data. We believe that this work shows an alternative research path in the pursuit of effective and efficient learning techniques for deep neural networks. This also opens the possibility of avoiding the use of pyramidal architectures commonly employed in DNNs, thus removing the computational burden caused by the additional units and reducing the dimensionality of the internal representations.

We additionally show that our proposal enables the use of Zero Initialization. The results are promising, and though further experimentation is still needed, they still manage to surpass Batch Normalization in terms of depth, width, and accuracy. Nevertheless, the modifications used to break the symmetry of constraints and units need further consideration in order to achieve the same performance than random initialization.

Despite this article provides no information about the dynamics of the training process using Separation Constraints, preliminary revision shows interesting properties. In particular, training displays slight instabilities which appear as the units/points are reactivated. Although this does not hinder the training process, further study is needed in order to guarantee a smoother convergence.

The extension of this work to other activation functions is still to be explored. However, we conjecture that in cases where the activation function display a flat region, e.g. ELU, tanh, or even sigmoid, the current proposal can be applied with minor changes.

Finally, while the separation constraints prevent the vanishing gradient effect, the *exploding gradient* problem still remains. Extending the Separation Constraint with an upper bound on the magnitudes of the pre-activation, similar to ϵ-insensitive loss, might address it. It could be also helpful to explore other activation functions whose gradient vanishes with high pre-activations, such as the logistic family.

REFERENCES

Martín Abadi, Ashish Agarwal, Paul Barham, Eugene Brevdo, Zhifeng Chen, Craig Citro, Greg S. Corrado, Andy Davis, Jeffrey Dean, Matthieu Devin, Sanjay Ghemawat, Ian Goodfellow, Andrew Harp, Geoffrey Irving, Michael Isard, Yangqing Jia, Rafal Jozefowicz, Lukasz Kaiser, Manjunath Kudlur, Josh Levenberg, Dandelion Mané, Rajat Monga, Sherry Moore, Derek Murray, Chris Olah, Mike Schuster, Jonathon Shlens, Benoit Steiner, Ilya Sutskever, Kunal Talwar, Paul Tucker, Vincent Vanhoucke, Vijay Vasudevan, Fernanda Viégas, Oriol Vinyals, Pete Warden, Martin Wattenberg, Martin Wicke, Yuan Yu, and Xiaoqiang Zheng. TensorFlow: Large-scale machine learning on heterogeneous systems, 2015. URL `https://www.tensorflow.org/`. Software available from tensorflow.org.

Stephen Boyd and Lieven Vandenberghe. *Convex Optimization*. Cambridge University Press, New York, NY, USA, 2004. ISBN 0521833787.

François Chollet et al. Keras. `https://keras.io`, 2015.

Corinna Cortes and Vladimir Vapnik. Support-vector networks. *Machine learning*, 20(3):273–297, 1995.

Scott C. Douglas and Jiutian Yu. Why relu units sometimes die: Analysis of single-unit error backpropagation in neural networks. *CoRR*, abs/1812.05981, 2018. URL `http://arxiv.org/abs/1812.05981`.

Xavier Glorot and Yoshua Bengio. Understanding the difficulty of training deep feedforward neural networks. In *In Proceedings of the International Conference on Artificial Intelligence and Statistics (AISTATS10). Society for Artificial Intelligence and Statistics*, 2010.

Xavier Glorot, Antoine Bordes, and Yoshua Bengio. Deep sparse rectifier neural networks. In Geoffrey Gordon, David Dunson, and Miroslav Dudk (eds.), *Proceedings of the Fourteenth International Conference on Artificial Intelligence and Statistics*, volume 15 of *Proceedings of Machine Learning Research*, pp. 315–323, Fort Lauderdale, FL, USA, 11–13 Apr 2011. PMLR. URL http://proceedings.mlr.press/v15/glorot11a.html.

Rachid Guerraoui et al. When neurons fail. In *2017 IEEE International Parallel and Distributed Processing Symposium (IPDPS)*, pp. 1028–1037. IEEE, 2017.

Seyyed Hossein Hasanpour, Mohammad Rouhani, Mohsen Fayyaz, Mohammad Sabokrou, and Ehsan Adeli. Towards principled design of deep convolutional networks: Introducing simpnet. *CoRR*, abs/1802.06205, 2018. URL http://arxiv.org/abs/1802.06205.

Kaiming He, Xiangyu Zhang, Shaoqing Ren, and Jian Sun. Delving deep into rectifiers: Surpassing human-level performance on imagenet classification. *CoRR*, abs/1502.01852, 2015a. URL http://arxiv.org/abs/1502.01852.

Kaiming He, Xiangyu Zhang, Shaoqing Ren, and Jian Sun. Deep residual learning for image recognition. *CoRR*, abs/1512.03385, 2015b. URL http://arxiv.org/abs/1512.03385.

Sepp Hochreiter. Untersuchungen zu dynamischen neuronalen netzen. *Diploma, Technische Universität München*, 91(1), 1991.

Sepp Hochreiter. Gradient flow in recurrent nets: the difficulty of learning long-term dependencies. 2001.

Gao Huang, Zhuang Liu, and Kilian Q. Weinberger. Densely connected convolutional networks. *CoRR*, abs/1608.06993, 2016. URL http://arxiv.org/abs/1608.06993.

Sergey Ioffe and Christian Szegedy. Batch normalization: Accelerating deep network training by reducing internal covariate shift. *CoRR*, abs/1502.03167, 2015. URL http://arxiv.org/abs/1502.03167.

Diederik P. Kingma and Jimmy Ba. Adam: A method for stochastic optimization. *CoRR*, abs/1412.6980, 2014. URL http://arxiv.org/abs/1412.6980.

Alex Krizhevsky. Learning multiple layers of features from tiny images. Technical report, 2009.

Yann LeCun and Corinna Cortes. MNIST handwritten digit database. 2010. URL http://yann.lecun.com/exdb/mnist/.

Yann LeCun, Sumit Chopra, and Raia Hadsell. A tutorial on energy-based learning. 2006.

Yann LeCun, Yoshua Bengio, and Geoffrey Hinton. Deep learning. *Nature*, 521(7553):436–444, May 2015. ISSN 0028-0836. doi: 10.1038/nature14539. URL http://dx.doi.org/10.1038/nature14539.

Zhuang Liu, Mingjie Sun, Tinghui Zhou, Gao Huang, and Trevor Darrell. Rethinking the value of network pruning. *CoRR*, abs/1810.05270, 2018. URL http://arxiv.org/abs/1810.05270.

Lu Lu, Yeonjong Shin, Yanhui Su, and George Em Karniadakis. Dying relu and initialization: Theory and numerical examples. *arXiv preprint arXiv:1903.06733*, 2019.

Andrew L. Maas. Rectifier nonlinearities improve neural network acoustic models. 2013.

Razvan Pascanu, Tomas Mikolov, and Yoshua Bengio. On the difficulty of training recurrent neural networks. In *Proceedings of the 30th International Conference on International Conference on Machine Learning - Volume 28*, ICML'13, pp. III–1310–III–1318. JMLR.org, 2013. URL http://dl.acm.org/citation.cfm?id=3042817.3043083.

P. Ramachandran, B. Zoph, and Q. V. Le. Swish: a Self-Gated Activation Function. *ArXiv e-prints*, October 2017.

Steven J Rennie, Vaibhava Goel, and Samuel Thomas. Annealed dropout training of deep networks. In *2014 IEEE Spoken Language Technology Workshop (SLT)*, pp. 159–164. IEEE, 2014.

Carles Riera and Oriol Pujol. Solving internal covariate shift in deep learning with linked neurons. *arXiv preprint arXiv:1712.02609*, 2017.

Wenling Shang, Kihyuk Sohn, Diogo Almeida, and Honglak Lee. Understanding and improving convolutional neural networks via concatenated rectified linear units. *CoRR*, abs/1603.05201, 2016. URL http://arxiv.org/abs/1603.05201.

Yeonjong Shin and George E. Karniadakis. Trainability and data-dependent initialization of over-parameterized relu neural networks. *CoRR*, abs/1907.09696, 2019. URL http://arxiv.org/abs/1907.09696.

Christian Szegedy, Wei Liu, Yangqing Jia, Pierre Sermanet, Scott E. Reed, Dragomir Anguelov, Dumitru Erhan, Vincent Vanhoucke, and Andrew Rabinovich. Going deeper with convolutions. *CoRR*, abs/1409.4842, 2014. URL http://arxiv.org/abs/1409.4842.

Mingxing Tan and Quoc V. Le. Efficientnet: Rethinking model scaling for convolutional neural networks. *CoRR*, abs/1905.11946, 2019. URL http://arxiv.org/abs/1905.11946.

Sergey Zagoruyko and Nikos Komodakis. Wide residual networks. *CoRR*, abs/1605.07146, 2016. URL http://arxiv.org/abs/1605.07146.

A APPENDIX

A.1 UNIT BASED AND POINT BASED SEPARATION CONSTRAINT EXPERIMENT

In order to justify the decision of combining `Sep-U` and `Sep-P` into `Sep-UP`, we provide Figure 5 showing the same experiment than Figure 1 for `Sep-U` and `Sep-U`. We find how although `Sep-U` is able to train deeper and thinner networks it suffers from inferior accuracy (see Figures 5a and 5c), requiring the use of the layer width increase technique. Contrarily, `Sep-P` is able to train without increasing the width from 1 to 40 layers deep, but it breaks down afterwards. Provided how complementary are their strengths and weaknesses, it is sensible to combine them, resulting in the superior performance (larger constant width area together with greater accuracy in higher depths) of `Sep-UP`, see Figures 1c and 1f.

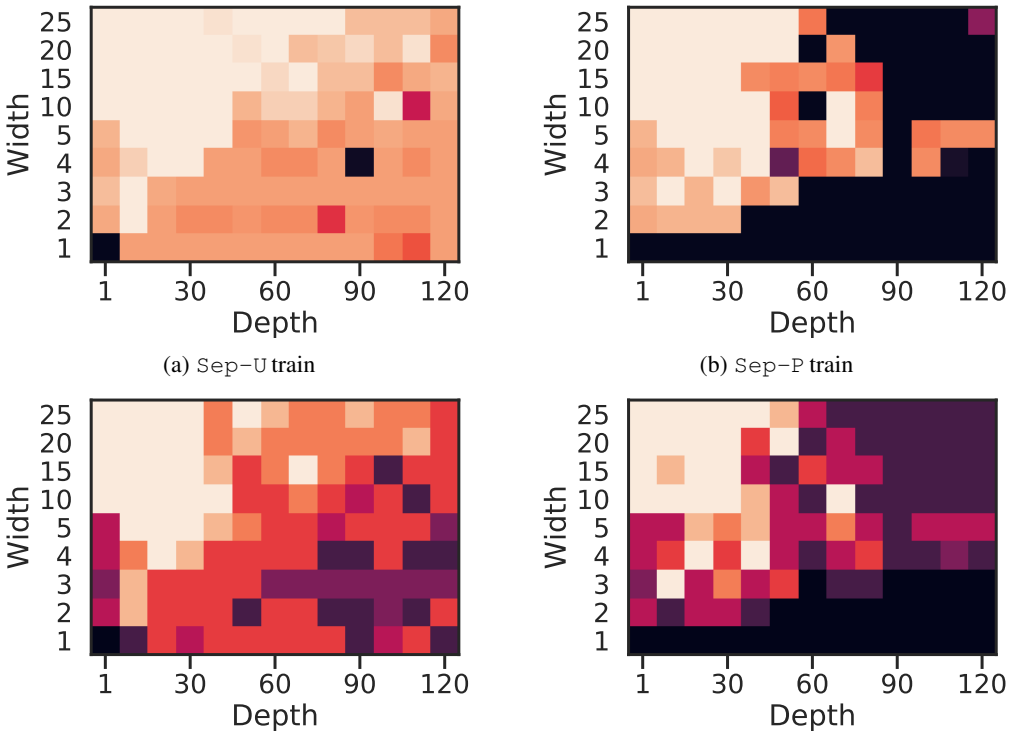

(a) `Sep-U` train

(b) `Sep-P` train

(c) `Sep-U` validation

(d) `Sep-P` validation

Figure 5: Depth vs width accuracy heatmap a for a grid of rectangular networks with width from 1 to 25 and depth from 1 to 120, trained using `Adam` with a learning rate of 0.01 in the `MOONS` dataset for 5000 epochs. The color shows the accuracy attained of each of the combinations of width and depth, with clear beige at 1 and black at 0.5. Notice how `Sep-U` enables train thinner and deeper networks (120 layers of single unit), but with reduced performance compared to `Sep-UP`. It also requires increasing the width of the layers in order to achieve perfect accuracy as `ReLU + BN`. Alternatively, `Sep-P` shows a constant width area between 1 and 40 layers, but its performance is much worse above. This justifies the decision of combining them both into `Sep-UP` to combine their strengths.